APPLIED AND ENVIRONMENTAL MICROBIOLOGY, Mar. 2008, p. 1869–1875 Vol. 74, No. 6
0099-2240/08/$08.00+0 doi:10.1128/AEM.02218-07

Direct Visualization of Spatial and Temporal Patterns of Antimicrobial Action within Model Oral Biofilms▽

Shoji Takenaka,[1]† Harsh M. Trivedi,[2] Audrey Corbin,[1] Betsey Pitts,[1] and Philip S. Stewart[1]*

Center for Biofilm Engineering, Montana State University–Bozeman, Bozeman, Montana,[1] and Colgate-Palmolive Technology Center, Piscataway, New Jersey[2]

Received 21 September 2007/Accepted 6 January 2008

A microscopic method for noninvasively visualizing the action of an antimicrobial agent inside a biofilm was developed and applied to describe spatial and temporal patterns of mouthrinse activity on model oral biofilms. Three species biofilms of *Streptococcus oralis*, *Streptococcus gordonii*, and *Actinomyces naeslundii* were grown in glass capillary flow cells. Bacterial cells were stained with the fluorogenic esterase substrate Calcien AM (CAM). Loss of green fluorescence upon exposure to an antimicrobial formulation was subsequently imaged by time-lapse confocal laser scanning microscopy. When an antimicrobial mouthrinse containing chlorhexidine digluconate was administered, a gradual loss of green fluorescence was observed that began at the periphery of cell clusters where they adjoined the flowing bulk fluid and progressed inward over a time period of several minutes. Image analysis was performed to quantify a penetration velocity of 4 μm/min. An enzyme-based antimicrobial formulation led to a gradual, continually slowing loss of fluorescence in a pattern that was qualitatively different from the behavior observed with chlorhexidine. Ethanol at 11.6% had little effect on the biofilm. None of these treatments resulted in the removal of biomass from the biofilm. Most methods to measure or visualize antimicrobial action in biofilms are destructive. Spatial information is important because biofilms are known for their structural and physiological heterogeneity. The CAM staining technique has the potential to provide information about the rate of antimicrobial penetration, the presence of tolerant subpopulations, and the extent of biomass removal effected by a treatment.

Direct time-lapse microscopic observation has proven to be an extremely powerful tool over the last decade in developing insight into the complex, spatially structured behaviors of microbial biofilms. This approach has revealed, for example, fluid flow patterns in the channels and interstices of heterogeneous biofilm structures (31), dynamic biomass movement and viscoelastic flow (17, 30), the contribution of cell migration to the formation of mushroom-like structures (18), transient patterns of gene expression (25, 37), the time course of diffusive penetration of solutes into biofilms (15, 24), and rapid motility of cells trapped in hollow biofilm cell clusters (14, 34).

There have been few applications of time-lapse microscopy to investigate the action of antimicrobial agents against biofilms (4, 11, 16). Most of the techniques used to assess the action of antimicrobial agents on biofilms involve sacrificial sampling followed by plating or endpoint staining. By these methods it is difficult to gain insight into spatiotemporal patterns because it is not possible to observe a single spot in time.

We have developed a microscopic method for noninvasively visualizing the action of an antimicrobial agent inside a biofilm. The first step in this method is to load bacterial cells with a fluorescent dye by incubating them with a fluorogenic esterase substrate (2, 26), in this case, Calcien AM (CAM). This uncharged, nonfluorescent substrate diffuses passively into the cytoplasm of the cell, where it is acted upon by ubiquitous native esterases. The result of the enzymatic transformation is a charged fluorescent product that is trapped inside cells with intact membranes by virtue of its charge. Bacteria stained in this way retain their fluorescence for several hours or longer, even after the CAM is removed. Now, when an antimicrobial agent is applied, permeabilization of the cell envelope that results can be visualized as the fluorescent dye leaks from the cell. Since many antimicrobial treatments eventually result in cell permeabilization or lysis (21), this is potentially a generic technique for monitoring antimicrobial action.

We describe here the development of the CAM staining technique and demonstrate that this technique can provide information about the time scale for antimicrobial agent penetration into biofilm, spatial differences in the relative susceptibility of microbial cells to antimicrobial attack, and removal of biomass from the biofilm.

MATERIALS AND METHODS

Bacteria and media. *Streptococcus oralis* ATCC 10557, *Streptococcus gordonii* ATCC 10558, and *Actinomyces naeslundii* ATCC 19039 were used in the present study. These organisms, which initiate colonization and coaggregate with each other on the tooth surface (19), were grown from frozen stocks in tryptic soy broth (TSB) containing 0.5% sucrose overnight at 37°C under anaerobic conditions with the GasPak EZ system (Becton Dickinson). Starter cultures were transferred into 10 ml of fresh, anaerobic sucrose-amended TSB and grown for 2 h (*S. gordonii*) or 4 h (other strains) at 37°C under aerobic conditions. The absorbance at 600 nm of all bacterial suspensions was adjusted to 0.05 prior to preparing inocula.

Biofilm reactor. The reactor system consisted of a carboy medium reservoir, peristaltic pump, glass capillary tube (Friedrich & Dimmock, Millville, NJ), and a carboy for waste. These components were connected by silicone tubing. The system has been described in detail in a prior publication (24). The nominal inside dimension of the glass tube was 0.9 mm square, and the wall thickness was

* Corresponding author. Mailing address: Center for Biofilm Engineering, Montana State University–Bozeman, Bozeman, MT 59717-3980. Phone: (406) 994-1960. Fax: (406) 994-6098. E-mail: phil_s@erc.montana.edu.

† Present address: Division of Cariology, Niigata University, Niigata, Japan.

▽ Published ahead of print on 25 January 2008.

0.17 ± 0.01 mm. The tube was approximately 10 cm long. The reactor system was sterilized by autoclaving.

Equal volumes of absorbance-adjusted suspensions of each of the three microorganisms prepared as described above were mixed, and 0.2 ml of this mixture was inoculated into a sterile glass capillary tube reactor. The inoculated solution was allowed to stand without flow for 2 h at 37°C under aerobic conditions. After 2 h, the flow of medium was initiated at a flow rate of 1 ml min^{-1}. The medium was 1/10 strength TSB containing 0.05% sucrose. Biofilms were allowed to develop for 20 h under continuous-flow conditions with incubation at 37°C.

Biofilm species composition characterization. A mature biofilm grown in a capillary was homogenized in phosphate buffer. This suspension was diluted in the same buffer and plated on two media: tryptic soy agar plus 5% sucrose and *Actinomyces* selective medium. After 48 h of growth in a CO_2 incubator, the colonies were counted. One milliliter of biofilm suspension was filtered through a polycarbonate membrane (0.22-mm pore size, 13 mm; Poretics Corp.). The cells were rinsed with 1% bovine serum albumin in phosphate-buffered saline-Tween solution. A dilution of antistreptococcal rabbit immunoglobulin G antibody (a gift from Rob Palmer) was introduced for 1 h, followed by rinsing with the bovine serum albumin solution. A 200-fold dilution factor of fluorescein isothiocyanate secondary antibody was added for 1 h, illuminating streptococci cells in green. Propidium iodide was used as a counterstain (15 min incubation) to reveal all cells in red fluorescence.

Microscopy, staining, and treatment. A mature biofilm grown in the capillary reactor was removed from the incubator to the benchtop, and subsequent processing and microscopy was conducted at ambient temperature of 23°C. Medium was flushed from the reactor by introducing a continuous flow of buffer containing 0.25 g of dipotassium phosphate and 0.5 g of sodium chloride per liter (pH 7.3). CAM (Molecular Probes/Invitrogen, Eugene, OR) was prepared to a concentration of 10 μg/ml in the same buffer by diluting a 500-μg/ml stock solution (in dimethyl sulfoxide) into buffer. The CAM solution was pumped into the capillary at a flow rate of 1 ml min^{-1} until it completely replaced the fluid in the capillary. The flow was stopped, and the biofilm was stained statically for 2 h. Excess stain was washed out by restoring the flow of buffer.

For microscope observation of biofilm, the capillary was placed in a holder (Biosurface Technologies, Bozeman, MT) that was mounted on the microscope stage. Biofilms were imaged on a Leica TCS-SP2 AOBS using an Ar-488 nm laser and a Leica/Spectra Physics MaiTai 2-photon system (Ti/Sapphire 780- to 920-nm infrared laser). The two-photon excitation option was used to reduce photobleaching. A ×63 0.9 NA water-immersion objective lens was used. The plane just under the glass ceiling of the capillary was brought into focus. That plane was also the bottom surface of a biofilm cluster. Image time series were collected at this single fixed height.

Biofilm was exposed to commercially available mouthrinses or treatment solutions under continuous flow at flow rate of 1 ml min^{-1}, and images were collected every 30 s for 20 min. The treatments used included: (i) buffer, as a control; (ii) 11.6% ethanol in water; and (iii) 0.12% chlorhexidine gluconate, as supplied in an alcohol-free formulation by GUM (Sunster Butler, Chicago, IL), and a commercial mouthrinse (Biotene), which contains lysozyme, lactoferrin, lactoperoxidase, glucose oxidase, and potassium thiocyanate (Laclede, Rancho Dominguez, CA). This concentration of ethanol was chosen because it is similar to concentrations found in some commercial mouthrinses. A treatment with a slurry of Colgate Total toothpaste (1 part paste and 3 parts water) was also used in duplicate experiments to demonstrate the potential of this technique to image the action of opaque treatments that disrupt the biofilm. The treatment time was approximately 5 min.

For imaging antimicrobial action, the 780-nm two-photon laser line was used for excitation and the fluorescent signal was detected in a green channel. Transmitted images of biofilms before and after exposure were collected in transmission mode with excitation from the 488-nm laser.

Two types of biofilm structures were examined. Isolated cell clusters in the central third of the capillary were analyzed to produce the data reported in Fig. 1, 2, and 5. Biofilm growing in the corner of the capillary was analyzed to produce the results reported in Fig. 3 and 4. We refer hereafter to these two types of biofilm structures as biofilm clusters and biofilm in the flow cell corner.

Image analysis. Images were analyzed in MetaMorph software (Universal Imaging Corp., Downington, PA). The overall effect of a treatment on biofilm clusters was assessed by tracking the green fluorescence intensity throughout the entire cluster in time. The boundary of the cell cluster was drawn in MetaMorph, and the integrated green pixel intensity inside this area was calculated by the software at each time step. These values were normalized by dividing them by the initial value of the integrated cluster intensity. Six biofilm clusters from six separate experiments were analyzed for each treatment condition.

Biofilm in the flow cell corner was analyzed to determine spatial patterns. The average fluorescence intensity at various depths (20, 40, 60, 80, and 100 μm) from the biofilm-bulk fluid interface was calculated and again normalized by dividing by the initial value of the intensity at that particular location. The region of analysis at each depth was a square that was 15 by 15 pixels or approximately 7 μm on a side. This analysis was performed five times for each treatment condition.

RESULTS

Heterogeneous biofilms formed in capillary reactors. After 24 h of growth in the capillary reactor, selective plating of biofilm dispersed from the reactor showed that the biofilm was composed mostly of streptococci. Both *S. oralis* and *S. gordonii* were present. There were approximately 1,000 times fewer *Actinomyces* than streptococci. The predominance of staphylococci was confirmed by staining of the dispersed biofilm cells with an anti-*Streptococcus* fluorescent antibody. Although *A. naeslundii* was a minor component of the mature biofilm, this microorganism was retained in the inoculum because inoculation with all three species resulted in better attachment and more rapid biofilm formation than when *A. naeslundii* was omitted.

In tests with pure cultures of planktonic cells, all three of the microbial species used in this investigation stained green when incubated with CAM. When three-species biofilms (Fig. 1A) were incubated with CAM for 2 h, bright green fluorescence developed throughout the biofilm (Fig. 1B). This fluorescence remained associated with biomass in the biofilm even after a continuous flow of buffer was initiated. The mean diameter of cell clusters used for analysis in the present study ranged from 75 to 111 μm.

When an antimicrobial mouthrinse, the active ingredient in which was chlorhexidine digluconate, was subsequently flowed into the reactor, a gradual loss of green fluorescence was observed (Fig. 1C to G). Fluorescence was lost first at the periphery of cell clusters adjoining the flowing bulk fluid (compare Fig. 1B and D). Loss of fluorescence progressed inward over a time period of several minutes. Even after 20 min of exposure, some spots of the biofilm remained bright. This sequence can be viewed as a movie (http://www.erc.montana.edu/Res-Lib99-SW/Movies/2007/07-M001.htm). In this and other time series of antimicrobial action, the loss of green fluorescence was radially symmetric. That is, fluorescence loss at the downstream and upstream edges of the cell cluster was the same.

Antimicrobial action visualized by the CAM staining technique can be quantified through image analysis. The fluorescent intensity averaged over the area of a cell cluster divided by the value of this average immediately prior to antimicrobial treatment was plotted against time. This ratio provides a way of tracking the integrated action of the antimicrobial over an entire cluster. This analysis was applied to biofilms treated with chlorhexidine, ethanol, and a commercial enzyme-based antimicrobial formulation called Biotene (Fig. 2). Untreated control biofilms retained most of their fluorescence during the 20 min observation period (Fig. 2A). The averaged fluorescence intensity after a 20-min control exposure was 97% of the initial intensity. Biofilms exposed to 11.6% ethanol for 20 min were also scarcely affected; the averaged fluorescent intensity after exposure to this alcohol was 96% of the initial intensity (Fig. 2B). Exposure to a solution containing chlorhexidine diglu-

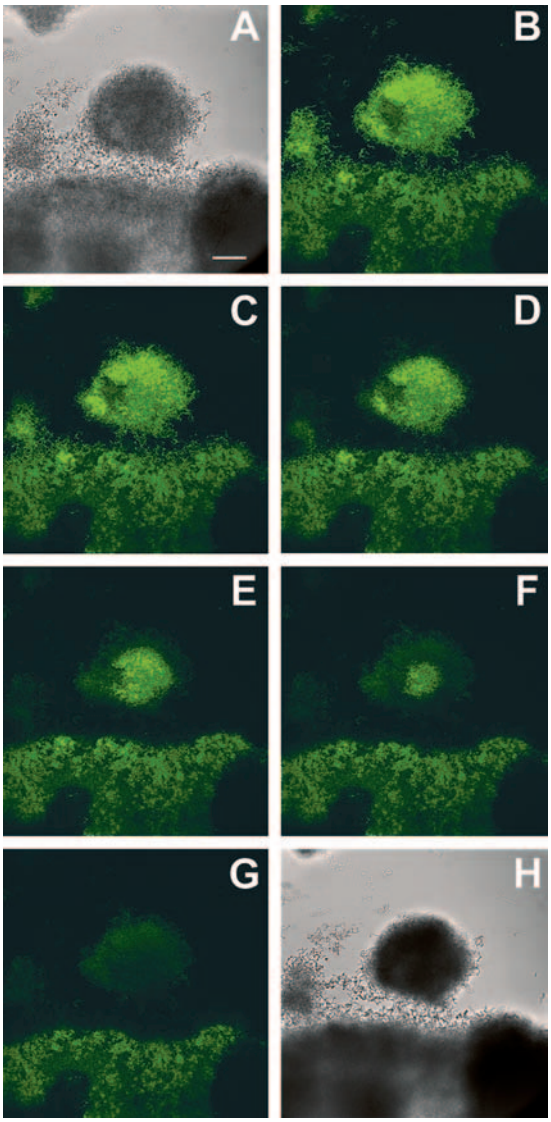

FIG. 1. Antimicrobial action of 0.12% chlorhexidine on oral biofilm stained with CAM (green). (A) Transmission image of the biofilm before treatment. (B) Staining observed in the biofilm immediately prior to the introduction of a 0.12% chlorhexidine solution (Gum commercial mouthrinse, alcohol free). (C to G) Progressive loss of fluorescence as the chlorhexidine penetrates the biofilm (for time points 90, 180, 270, 360, and 450 s, respectively). (H) Transmission image of the biofilm after treatment. Scale bar, 30 μm.

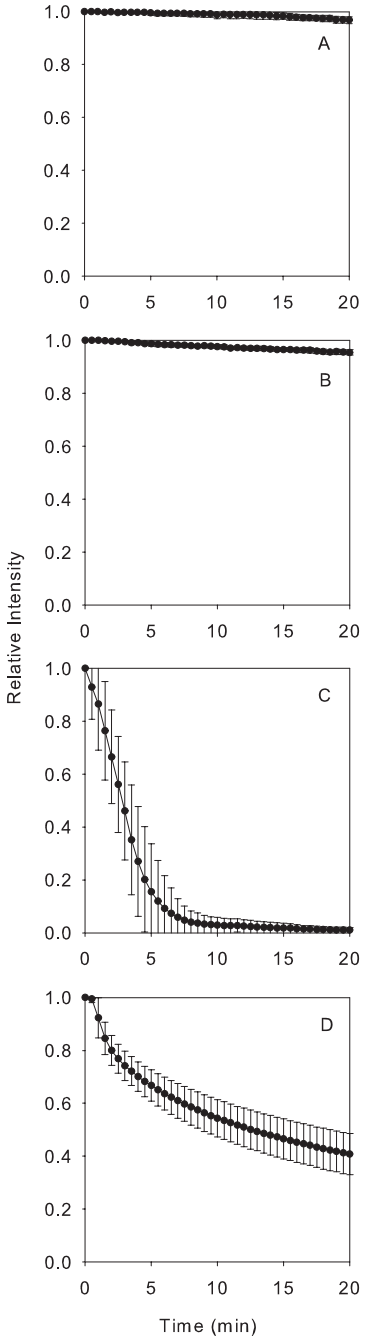

FIG. 2. Antimicrobial action against model oral biofilm cluster as determined by loss of fluorescence after CAM staining. The *y*-axis is the fluorescence intensity integrated over a field of view and normalized to the initial value. Four panels present the results obtained with the following treatments: untreated control (A), 11.6% ethanol (B), 0.12% chlorhexidine (C), and Biotene (D). Each data point represents the mean, and error bars denote the standard deviations ($n = 6$).

conate almost entirely eliminated fluorescence after 20 min (Fig. 2C). Exposure to Biotene reduced the averaged fluorescence to ca. 40% of the initial value (Fig. 2D).

The analysis reported in Fig. 2 does not provide any spatial information and in particular does not convey the progressive penetration that is obvious in Fig. 1. To capture this information, the fluorescence intensity at selected spots located at fixed depths from the surface of a biofilm in the flow cell corner was compared to the initial fluorescence intensity at these same locations (Fig. 3). This analysis generated a family of curves, one curve for each depth, that allows the time-dependent penetration to be discerned.

Application of this analysis to the action of chlorhexidine against biofilm in the flow cell corner (Fig. 3B) revealed a distinctive pattern. After a delay in which there was little loss of fluorescence, fluorescence diminished rapidly to background levels. The duration of the delay phase depended on the depth in the biofilm, with larger delays for greater depths.

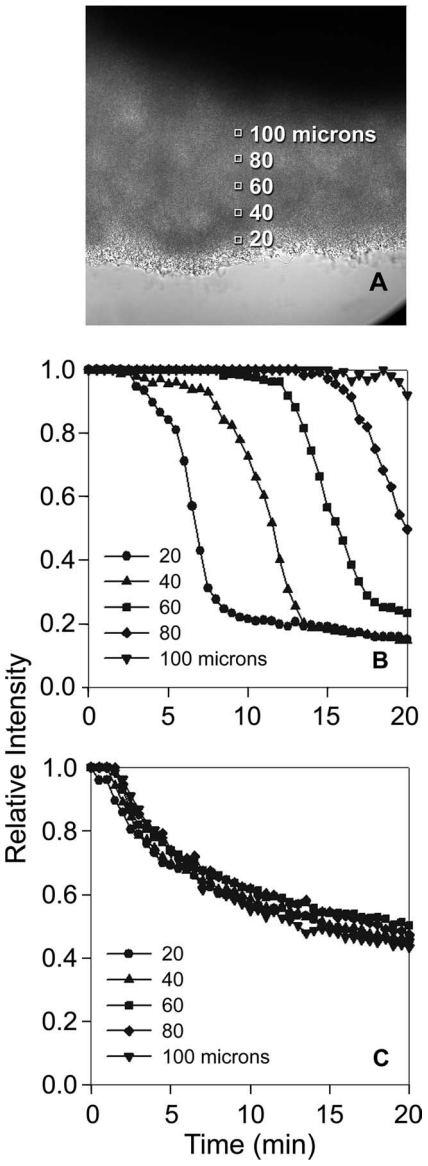

FIG. 3. Antimicrobial action against model oral biofilm in the corner of flow cells as determined by loss of fluorescence after CAM staining. (A) Typical regions of analysis in a biofilm in the flow cell corner. In panels B and C, the *y* axis is the fluorescence intensity at a particular depth in the biofilm divided by the initial fluorescence intensity at the same location. The depth from the biofilm-bulk fluid interface is indicated in microns. Shown are representative results for 0.12% chlorhexidine (B) and Biotene (C).

The rate of loss of fluorescence during the loss phase was similar at different depths. At the largest depth measured of 100 μm, no change of fluorescence was detected during the 20-min observation period. An entirely different pattern was revealed during treatment with Biotene (Fig. 3C). With this mouthrinse, a gradual, continually slowing loss of fluorescence was observed. Some of the curves suggest a possible delay period (e.g., at 100 μm depth), but the delay is less than 2 min. The curves at different depths are all similar, suggesting that penetration is not the rate controlling process with this formulation.

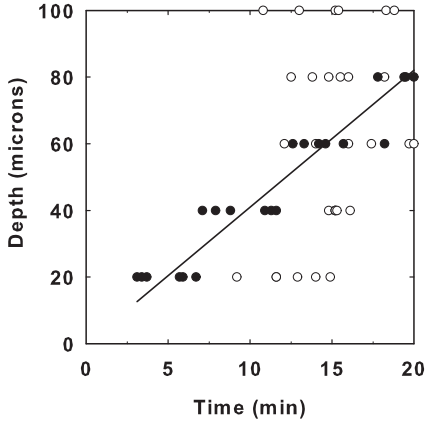

FIG. 4. Penetration of antimicrobial action in model oral biofilm in the corner of flow cells during treatment with 0.12% chlorhexidine (●) or Biotene (○). The solid line derives from a least-squares fitted analysis of the chlorhexidine data; the slope of this line is 4.1 μm/min. The data are from six independent experiments.

To further define the rate of penetration of antimicrobial activity, we calculated, at various locations in the biofilm, the time required to reach 50% of the initial fluorescence intensity. By plotting the depth of each spot from the biofilm surface as a function of this time, the penetration of the antimicrobial activity can be described (Fig. 4). In the case of chlorhexidine exposure, the progressive delivery of permeabilizing activity is roughly linear. After 20 min of exposure, the front of antimicrobial activity had traveled approximately 80 μm. The slope of this plot has units of velocity. For chlorhexidine, the average penetration velocity was 4.1 μm min^{-1}. In the case of Biotene exposure, the 50% antimicrobial action time was nearly the same, approximately 15 min, independent of the depth of the spot being observed. The interpretation of these data is that the penetration time is less than 15 min at all locations. It does not make sense to calculate a velocity in this case because the data do not tend to the origin for small depths.

During treatment with buffer, aqueous ethanol, and Biotene, no change in biofilm structure could be discerned. Treatment with chlorhexidine caused a slight contraction of the biofilm, and the biofilm became less translucent as a result (compare Fig. 1A and H). The contraction in cluster diameter after treatment with chlorhexidine was ca. 10% or less. There was no evidence that any of the treatments caused removal or detachment of biomass from the biofilm.

To illustrate the potential of this technique to examine the effects of treatments that block light, we treated a capillary reactor biofilm with a toothpaste slurry. The slurry was opaque, and thus it was not possible to visualize the biofilm by transmission mode microscopy during the treatment period. It remained possible to visualize the loss of fluorescence from CAM-stained bacteria as shown in Fig. 5B to G. In addition to causing loss of fluorescence, indicating antimicrobial action, the toothpaste slurry removed a substantial amount of biomass. The cell cluster under observation in Fig. 5 was completely removed from the surface of the glass capillary after approximately 3 min of exposure to the flowing slurry (compare Fig. 5A and H). This removal could be discerned by the discrete loss of residual fluorescence associated with the bio-

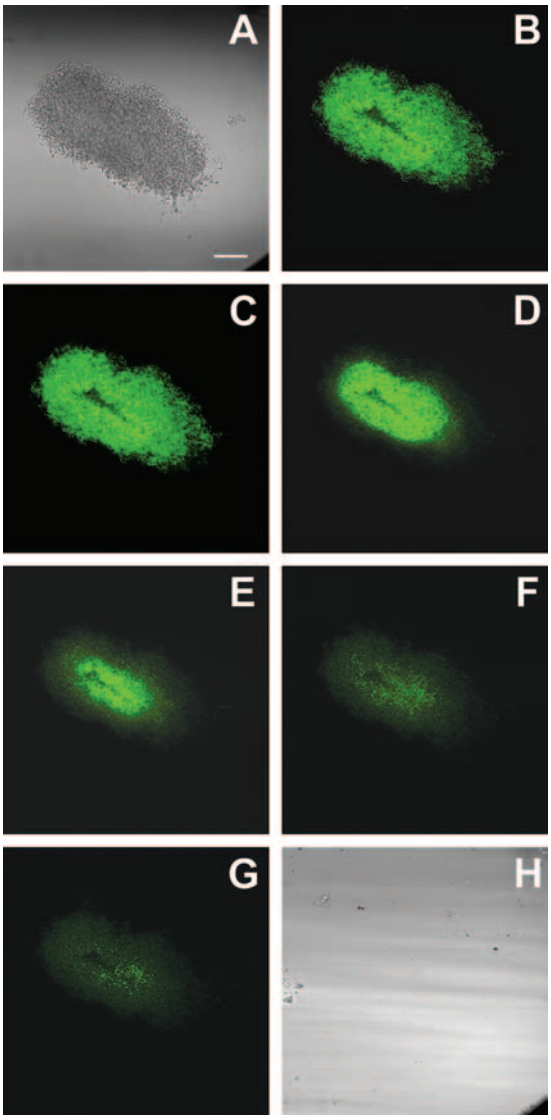

FIG. 5. Action of Colgate Total toothpaste slurry on model oral biofilm stained with CAM (green). (A) Transmission image of the biofilm before treatment. (B) Staining observed in the biofilm immediately prior to the introduction of a toothpaste slurry. Panels C to G show the progressive loss of fluorescence as unidentified components of the formulation penetrates the biofilm (time points 25, 30, 35, 40, and 45 s, respectively). (H) Transmission image of the biofilm after treatment. Scale bar, 30 μm.

mass from one image to the next. The removal was visually confirmed when the slurry was replaced with buffer and the capillary was imaged in transmission mode again (Fig. 5H). In a duplicate experiment of this type (results not shown), a similar loss of fluorescence was observed, but the biofilm cell cluster was not removed. At the end of the 3-min treatment period, particulates could be seen stuck to the biofilm matrix.

DISCUSSION

Most methods to measure or visualize antimicrobial action in biofilms are destructive. In the conventional viable plate count determination, for example, a biofilm-covered coupon is scraped or sonicated, and the resulting suspension of cells is diluted and plated. This processing destroys spatial information and is obviously incompatible with observing a single location in time. Another popular approach for evaluating antimicrobial efficacy against biofilms is the commercial viability staining kit BacLight Live/Dead (6, 12, 32). Staining with a fluorogenic redox dye has also been used to evaluate activity patterns (13, 27). Staining with these probes preserves spatial information for subsequent microscopic examination, but because the stains harm the cell, this technique is incompatible with observing a specific biofilm location at multiple time points.

Spatial information is important because biofilms are known for their structural and physiological heterogeneity (25, 29, 35). Localized niches in the biofilm may exhibit differing responses to antimicrobial exposure. Two striking examples of this result have recently been reported for antimicrobial challenges against *Pseudomonas aeruginosa* biofilms (11, 16). For example, while tobramycin preferentially kills cells around the perimeter of cell clusters, gallium has exactly the reverse effect: cells in the interior of the biofilm are killed (16). These two studies both made use of *P. aeruginosa* tagged with a green fluorescent protein, which in effect "stains" all of the cells green. Propidium iodide was used to label cells that had compromised membrane integrity; these cells took up the dye and appeared red.

Temporal information is important because it can provide clues about the protective mechanisms. Modeling studies have suggested that the time course of biofilm killing is likely to be nonlinear. For example, when a tolerant subpopulation is present, the shape of the killing curve will be concave up, and when a reaction-diffusion interaction limits the rate of access of the antimicrobial agent into the biofilm the shape of the killing curve will be concave down (7–9). Based on this analysis, one would predict that chlorhexidine is penetration limited through a reaction-diffusion interaction (Fig. 3B), whereas Biotene is limited by phenotypic tolerance (Fig. 3C). In any case, different shapes of inactivation curves probably imply different rate-limiting processes.

As illustrated in Fig. 3B and 4, the fluorescence assay for cell permeability developed in this project can also provide information about the penetration of the antimicrobial agent into the biofilm. In the experiments presented in these figures, the penetration of chlorhexidine, a common antimicrobial constituent of mouthrinses, can be inferred. The loss of fluorescence in the biofilm occurs at similar rates at the surface of the biofilm as it does at a location near the center for a cell cluster. The apparent velocity at which chlorhexidine penetrated into the biofilm can be estimated from these data and was approximately 4 $\mu m\ min^{-1}$. These data show that chlorhexidine acts rapidly on cells once it reaches them, but it does require a relatively long time to reach the interior of the biofilm. The data allow the delay in antimicrobial action to be quantified. The shapes of these penetration curves imply an interaction between chlorhexidine and the biofilm, perhaps sorption of the antimicrobial to cells or matrix polymers, that results in its retardation.

All of the observations of antimicrobial action reported here are qualitatively consistent with symmetry of action on biofilm cell clusters. That is, the antimicrobials appear to act on the

upstream, downstream, and lateral aspects of the cell cluster in a similar way. This observation supports the contention that inside cell clusters solute transport occurs exclusively by diffusion (24, 29). If convective transport were significant, one would expect to see enhanced action of the antimicrobial agent at the upstream edge of the cell cluster in comparison to the downstream edge.

The penetration of antimicrobial activity, as judged by CAM fluorescence loss, was more rapid in biofilm cell clusters than it was in biofilm in the corner of flow cells. This is probably a reflection of both greater accumulation of biomass in the corners of flow cells (20), as well as reduced fluid velocities, and therefore reduced mass transport rates, in the corners of capillaries compared to the mid points of flow cell walls.

Biofilm structure was not much affected by any of the treatments. Treatments with chlorhexidine and ethanol may have resulted in a slight contraction of the biofilm. No removal of biomass was observed in control, chlorhexidine, Biotene, or ethanol exposures. In one of the two experiments with a toothpaste slurry, the cell cluster under observation was entirely removed from the glass substratum. This is likely a result of much higher viscosity of the toothpaste slurry in comparison to the antimicrobial solutions. A higher viscosity means that the shear and normal forces applied to the biofilm by the moving fluid will be higher.

Antimicrobial mouthrinses are an effective complement to mechanical oral hygiene (5). Of the antimicrobial solutions tested in this investigation, chlorhexidine is the active agent that has been most extensively studied, for example, in vitro (10, 12, 23), using an in situ oral biofilm model (3), and through clinical studies (1, 5, 22). These studies generally show that chlorhexidine is an effective antimicrobial agent. Our results indicate rapid action by chlorhexidine once it has penetrated, but raise the issue of relatively slow penetration of chlorhexidine. Components of the Biotene mouthrinse such as lysozyme, lactoferrin, and peroxidase, which are innate human salivary defense proteins, have also been shown to exert antimicrobial activity against a number of bacterial, viral, and fungal pathogens in vitro (33). At the concentration we tested of 11.6%, ethanol had little effect on a model oral biofilm. This result is in agreement with a report by Sissons et al. (28), who reported that 10% ethanol had almost no inhibitory effect on microcosm dental plaque. Similarly, Yang et al. (36) found that ethanol concentrations below 20% did not demonstrate significant inhibition against a polymicrobial oral biofilm.

We conclude with a few cautionary remarks about the relationship between fluorescence loss as measured by our technique and viability. The loss of fluorescence from a CAM-stained cell indicates that the cell has been rendered more permeable, but this does not necessarily mean that the cell has been killed. Conversely, the retention of fluorescence in a CAM-stained cell after treatment with an antimicrobial agent indicates that cell permeability has not been compromised but this does not mean that the cell is still alive. Developing a correlation between CAM fluorescence loss and viability by colony formation or cell growth would require experimental data for each antimicrobial of interest. This same limitation is true of other techniques that assess cell permeability, such as the commercial BacLight Live/Dead kit.

A technique for visualizing action on biofilm was developed in the present study in the context of oral biofilm control by antimicrobial mouthrinses. We anticipate that this technique can also be successfully adapted to investigate antimicrobial action in other biofilm systems.

ACKNOWLEDGMENT

This study was supported in part by Colgate-Palmolive.

REFERENCES

1. **Arweiler, N. B., N. Boehnke, A. Sculean, E. Hellwig, and T. M. Auschill.** 2006. Difference in efficacy of two commercial 0.2% chlorhexidine mouthrinse solutions: a 4-day plaque re-growth study. J. Clin. Periodontol. **33:**334–339.
2. **Auschill, T. M., N. B. Artweiler, L. Netuschil, M. Brecx, E. Reich, and A. Sculean.** 2001. Spatial distribution of vital and dead microorganisms in dental biofilms. Arch. Oral Biol. **46:**471–476.
3. **Auschill, T. M., N. Hein, E. Hellwig, M. Follo, A. Sculean, and N. B. Arweiler.** 2005. Effect of two antimicrobial agents on early in situ biofilm formation. J. Clin. Periodontol. **32:**147–152.
4. **Banin, E., K. M. Brady, and E. P. Greenberg.** 2006. Chelator-induced dispersal and killing of *Pseudomonas aeruginosa* cells in a biofilm. Appl. Environ. Microbiol. **72:**2064–2069.
5. **Barnett, M. L.** 2006 The rationale for the daily use of an antimicrobial mouthrinse. JADA **137:**16S–21S.
6. **Bjarnsholt, T., P. O. Jensen, M. Burmolle, M. Hentzer, J. A. J. Haagensen, H. P. Hougen, H. Calum, K. G. Madsen, C. Moser, S. Molin, N. Hoiby, and M. Givskov.** 2005. *Pseudomonas aeruginosa* tolerance to tobramycin, hydrogen peroxide and polymorphonuclear leukocytes is quorum-sensing dependent. Microbiology **151:**373–383.
7. **Cogan, N. G.** 2006. Effects of persister formation on bacterial response to dosing. J. Theor. Biol. **238:**694–703.
8. **Cogan, N. G., R. Cortez, and L. Fauci.** 2005. Modeling physiological resistance in bacterial biofilms. Bull. Math. Biol. **67:**831–853.
9. **Dodds, M. G., K. J. Grobe, and P. S. Stewart.** 2000. Modeling biofilm antimicrobial resistance. Biotechnol. Bioeng. **68:**456–465.
10. **Guggenheim, B., E. Giertsen, P. Schüpback, and S. Shapiro.** 2001. Validation of an in vitro biofilm model of supragingival plaque. J. Dent. Res. **80:**363–371.
11. **Haagensen, J. A. J., M. Klausen, R. K. Ernst, S. I. Miller, A. Folkesson, T. Tolker-Nielsen, and S. Molin.** 2007. Differentiation and distribution of colistin- and sodium dodecyl sulfate-tolerant cells in *Pseudomonas aeruginosa* biofilms. J. Bacteriol. **189:**28–37.
12. **Hope, C. K., and M. Wilson.** 2004. Analysis of the effects of chlorhexidine on oral biofilm vitality and structure based on viability profiling and an indicator of membrane integrity. Antimicrob. Agents Chemother. **48:**1461–1468.
13. **Huang, C.-T., F. P. Yu, G. A. McFeters, and P. S. Stewart.** 1995. Nonuniform spatial patterns of respiratory activity within biofilms during disinfection. Appl. Environ. Microbiol. **61:**2252–2256.
14. **Hunt, S. M., E. M. Werner, B. Huang, M. A. Hamilton, and P. S. Stewart.** 2004. Hypothesis for the role of nutrient starvation in biofilm detachment. Appl. Environ. Microbiol. **70:**7418–7425.
15. **Jefferson, K. K., D. A. Goldmann, and G. B. Pier.** 2005. Use of confocal microscopy to analyze the rate of vancomycin penetration through *Staphylococcus aureus* biofilms. Antimicrob. Agents Chemother. **49:**2467–2473.
16. **Kaneko, Y., M. Thoendel, O. Olakanmi, B. E. Britigan, and P. K. Singh.** 2007. The transition metal gallium disrupts *Pseudomonas aeruginosa* iron metabolism and has antimicrobial and antibiofilm activity. J. Clin. Investig. **117:**877–888.
17. **Klapper, I., C. J. Rupp, R. Cargo, B. Purevdorj, and P. Stoodley.** 2002. Viscoelastic fluid description of bacterial biofilm material properties. Biotechnol. Bioeng. **80:**289–296.
18. **Klausen, M., A. Aaes-Jorgensen, S. Molin, and T. Tolker-Nielsen.** 2003. Involvement of bacterial migration in the development of complex multicellular structures in *Pseudomonas aeruginosa* biofilms. Mol. Microbiol. **50:**61–68.
19. **Kolenbrander, P. E., R. N. Andersen, D. S. Blehert, P. G. Egland, J. S. Foster, and R. J. Palmer.** 2002. Communication among oral bacteria. Microbiol. Mol. Biol. Rev. **66:**486–505.
20. **Kuehn, M., M. Hausner, H.-J. Bungartz, M. Wagner, P. A. Wilderer, and S. Wuertz.** 1998. Automated confocal laser scanning microscopy and semiautomated image processing for analysis of biofilms. Appl. Environ. Microbiol. **64:**4115–4127.
21. **Maillard, J.-Y.** 2002 Bacterial target sites for biocide action. J. Appl. Microbiol. Symp. Suppl. **92:**16S–27S.
22. **Mei, H. C., D. J. White, J. Atema-Smit, E. Belt-Gritter, and H. J. Busscher.** 2006. A method to study sustained antimicrobial activity of rinse and dentrifice components on biofilm viability in vivo. J. Clin. Periodontol. **33:**14–20.
23. **Pratten, J., and M. Wilson.** 1999. Antimicrobial susceptibility and composition of microcosm dental plaques supplemented with sucrose. Antimicrob. Agents Chemother. **43:**1595–1599.
24. **Rani, S. A., B. Pitts, and P. S. Stewart.** 2005. Rapid diffusion of fluorescent

tracers into *Staphylococcus epidermidis* biofilms visualized by time lapse microscopy. Antimicrob. Agents Chemother. **49:**728–732.
25. **Rani, S. A., B. Pitts, H. Beyenal, R. A. Veluchamy, Z. Lewandowski, K. Buckingham-Meyer, and P. S. Stewart.** 2007. Spatial patterns of DNA replication, protein synthesis and oxygen concentration within bacterial biofilms reveal diverse physiological states. J. Bacteriol. **189:**4223–4233.
26. **Salih, H. R., L. Husfeld, and D. Adam.** 2000. Simultaneous cytofluorometric measurement of phagocytosis, burst production and killing of human phagocytes using *Candida albicans* and *Staphylococcus aureus* as target organisms. Clin. Microbiol. Infect. **6:**251–258.
27. **Schaule, G., H.-C. Flemming, and H. F. Ridgway.** 1993. Use of 5-cyano-2,3-ditolyl tetrazolium chloride for quantifying planktonic and sessile respiring bacteria in drinking water. Appl. Environ. Microbiol. **59:**3850–3857.
28. **Sissons, C. H., L. Wong, and T. W. Cutress.** 1996. Inhibition by ethanol of the growth of biofilm and dispersed microscosm dental plaques. Arch. Oral Biol. **41:**27–34.
29. **Stewart, P. S.** 2003. Diffusion in biofilms. J. Bacteriol. **185:**1485–1491.
30. **Stoodley, P., R. Cargo, C. J. Rupp, S. Wilson, and I. Klapper.** 2002. Biofilm material properties as related to shear-induced deformation and detachment phenomena. J. Ind. Microbiol. Biotechnol. **29:**361–367.
31. **Stoodley, P., D. de Beer, and Z. Lewandowski.** 1994. Liquid flow in biofilm systems. Appl. Environ. Microbiol. **60:**2711–2716.
32. **Teitzel, G. M., and M. R. Parsek.** 2003. Heavy metal resistance of biofilm and planktonic *Pseudomonas aeruginosa*. Appl. Environ. Microbiol. **69:**2313–2320.
33. **Tenovuo, J.** 2002. Clinical applications of antimicrobial host proteins lactoperoxidase, lysozyme, and lactoferrin in xerostomia: efficacy and safety. Oral Dis. **8:**23–29.
34. **Tolker-Nielsen, T., U. C. Brinch, P. C. Ragas, J. B. Andersen, C. S. Jacobsen, and S. Molin.** 2000. Development and dynamics of *Pseudomonas* sp. biofilms. J. Bacteriol. **182:**6482–6489.
35. **Xu, K. D., P. S. Stewart, F. Xia, C.-T. Huang, and G. A. McFeters.** 1998. Spatial physiological heterogeneity in *Pseudomonas aeruginosa* biofilm is determined by oxygen availability. Appl. Environ. Microbiol. **64:**4035–4039.
36. **Yang, Y., P. K. Sreenivasan, R. Subramanyam, and D. Cummins.** 2006. Multiparameter assessments to determine the effects of sugars and antimicrobials on a polymicrobial oral biofilm. Appl. Environ. Microbiol. **72:**6734–6742.
37. **Yarwood, J. M., D. J. Bartels, E. M. Volper, and E. P. Greenberg.** 2004. Quorum sensing in *Staphylococcus aureus* biofilms. J. Bacteriol. **186:**1838–1850.